Title

REACTION RATES IN PREMIXED IURBULENT FLAMES AND THEIR RELEVANCE TO THE TURBULENT BURNING SPEED

Authors

Cheng, R.K.
Shepherd, I.G.
Talbot, L.

Publication Date

1987-12-01

Lawrence Berkeley Laboratory
UNIVERSITY OF CALIFORNIA

APPLIED SCIENCE DIVISION

To be presented at the 22nd International Symposium on Combustion, Seattle, WA, August 15–19, 1988, and to be published in the Proceedings

Reaction Rates in Premixed Turbulent Flames and Their Relevance to the Turbulent Burning Speed

R.K. Cheng, I.G. Shepherd, and L. Talbot

December 1987

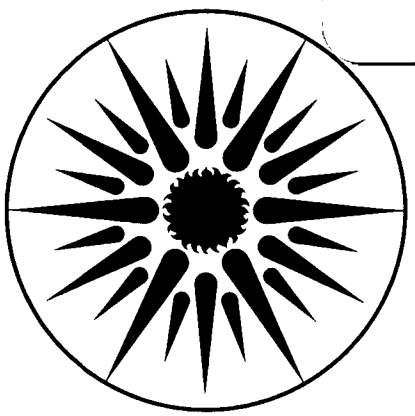

APPLIED SCIENCE DIVISION

Prepared for the U.S. Department of Energy under Contract Number DE-AC03-76SF00098.

DISCLAIMER

Reaction Rates in Premixed Turbulent Flames and their Relevance to the Turbulent Burning Speed

R. K. Cheng, I. G. Shepherd, and L. Talbot

Applied Science Division
Lawrence Berkeley Laboratory,
Berkeley CA 94720

Corresponding Author

Dr. R. K. Cheng
B29C Lawrence Berkeley Laboratory
1 Cyclotron Rd.
Berkeley, CA 94720

Subjects:

(30) Turbulent Reacting Flow
(23) Propagation Rates
(8) Experimental Methods

ABSTRACT

An experimental procedure to measure the local reaction rate, $\overline{w}$, in premixed turbulent flames is presented. It utilizes the flame crossing frequency sub-model for the reaction rate formulated by Bray-Champion-Libby (BCL) for turbulent flames with unstrained or equally strained flamelets. The experiments involve measuring the flame crossing frequencies and the conditioned mean velocity of two components using respectively Mie scattering and two color LDA techniques. A method of analysis has also been developed to deduce the turbulent burning speed from $\overline{w}$. The turbulent/laminar burning speed ratio is obtained by integrating the reaction rates measured along 2D mean Lagrangian flowlines through the flame brush. The flowlines are traced automatically using feedback control for positioning the LDA probe. The method has been applied to study five v-flames and four large Bunsen type conical flames. The distributions of $\overline{w}$ are well predicted by the BCL model. The turbulent flame speed results based on $\overline{w}$ are in excellent agreement with those obtained by the conventional flame orientation method. The main advantage of using this method to determine the turbulent burning speed is that the uncertainties are lowered. Furthermore, it can be applied successfully to flames with complex geometries such as the flame tip region of a conical flame.

INTRODUCTION

Recent advances in experimental and theoretical investigations of premixed turbulent flames have significantly improved the understanding of the velocity and scalar fields[1-9]. However, progress in quantifying and predicting the increase in burning rate with turbulence characteristics is still lagging. One of the reasons is that, to date, the most convenient means to express the increase in burning rate is by the use of the turbulent burning speed, S_T. The large uncertainties associated with determining S_T using the flame orientation method are well known. In many cases the results have been shown to be rather meaningless[10,11]. Consequently, reliable S_T data has only be obtained in configurations specially designed to reduce the uncertainties[9,12].

In theoretical models, S_T is either calculated (Anand and Pope[4]) or used as an input to predict mean properties within the flame brush [1,2]. However, its functional relation with the mean reaction rate $\overline{w}$, which requires modeling closure, remains largely unexplored by experiments. The model for $\overline{w}$ is usually expressed in terms of the length scale of the velocity field, viscous or scalar dissipation and an empirical constant. More recently Bray, Libby and Moss (BLM[1], and BL[2]) have based their models on the mean flame crossing frequencies, ν. The most significant feature of the crossing frequency concept is that ν can be measured directly in experiments using simple laser techniques. Their latest model (Bray, Champion and Libby (BCL)[13]), which provides the theoretical basis for this work, indicates a convenient means to

investigate $\overline{w}$ and evaluate its relevance to S_T. The significance for theoretical developments is that the $\overline{w}$ and S_T relationship could be used to validate the physical significance of this model and provide further insight for closing the chemical source term.

In this paper, the reaction rates as defined in BCL in five rod-stabilized v-flames and four large Bunsen conical flames were obtained by experimental measurements of ν,and $\overline{c}$, and conditioned and unconditioned two component velocities. A method of analysis is developed to evaluate turbulent/laminar speed ratio from the $\overline{w}$ data thus providing a novel means to determine S_T based on measurements of the local reaction rates as defined in BCL, which can be related to the turbulent burning speed. The S_Ts determined by this method are compared with those measured directly in the stagnation flow stabilized flames [9] and in the v-flames[10]. The physical implication of the results and comparison with the BML, BL, BCL models are discussed.

METHOD OF ANALYSIS

The Bray-Libby-Moss model (e.g. Ref. 1,2) of turbulent combustion is based on the flamelet concept which treats the turbulent flame region as consisting of a thin wrinkled fluctuating flame interface which separates the the unburned reactants from the burned products. Under the fast chemistry assumption, this model represents scalar quantities by a single progress variable, c. The second and third order turbulent transport terms can then be expressed in terms of c and the conditioned velocities in the reactants and products zones U_r,U_p. Since c has a value of 0 in the reactants and 1 in the reactants, a stationary probe measuring some scalar quantity detects only the burned and the unburned states and has an output similar to a random telegraph signal (Fig. 1). Each jump from 0 to 1 or vise versa represents the passage of a flame front. The passage times of reactants and products 'packets', t_r,t_p, can then be derived by specifying a signal threshold. The mean flame crossing frequency, ν and mean progress variable $\overline{c}$ are accordingly

$$\nu(x) = \frac{2}{\overline{t}_r(x) + \overline{t}_p(x)} \tag{1}$$

and

$$\bar{c}(x) = \frac{\bar{t}_p(x)}{\bar{t}_r(x) + \bar{t}_p(x)} \tag{2}$$

The model expresses the reaction rate $\bar{w}$ by a rather simple equation $\bar{w}(x) = w_f(x)\nu(x)$ where w_f is the mean rate of creation of products at each crossing. The reaction rate is the source term in the products mass conservation equation.

$$\frac{\partial}{\partial x}\bar{\rho}\tilde{u}\tilde{c} + \frac{\partial}{\partial y}\bar{\rho}\tilde{v}\tilde{c} + \frac{\partial}{\partial x}\overline{\rho u''c''} + \frac{\partial}{\partial y}\overline{\rho v''c''} = \bar{w} \tag{3}$$

By further assuming that the flame sheets consist of unstrained or equally strained laminar flamelets, i.e. the propagation speed of the flamelets is constant, BCL[13] models w_f as $w_f = \rho_r S_L/U_n$ such that

$$\bar{w} = \frac{\rho_r S_L \nu(x)}{U_n(x)} \tag{4}$$

where S_L is the laminar burning speed of the flamelet and U_n is the mean crossing speed of the flamelet in a laboratory frame. This expression does not contain empirical constants and all the parameters can be measured conveniently using laser diagnostic methods. The most significant feature, however, is its simple relationship to the turbulent burning speed.

For a one dimensional flame and along streamlines through 2-D flames, Eq. (3) reduces to

$$\frac{\partial}{\partial \xi}(\bar{\rho}\tilde{u}\tilde{c} + \overline{\rho u''c''}) = \bar{w} \tag{5}$$

where ξ is the co-ordinate normal to a 1-D flame or along the streamline of a 2-D flame. Integrating from $\xi = 0 \rightarrow \infty$ determines the overall creation rate of the products or the consumption rate of reactants through the turbulent flame brush i.e. the turbulent burning rate. By analogy to the laminar burning rate $\rho_r S_L$, the turbulent burning rate is $\rho_r S_T$. Recalling that the definition of S_T using the mass flow rate $\dot{m}$ through a streamtube is $\dot{m} = \rho_r S_L A_L = \rho_r S_T A_T$ where A_L is the area of the wrinkled flamelets and A_T is the effective cross-sectional area of the stream tube [11], the integral is then

$$\int_0^\infty \bar{w}\, d\xi = \rho_r S_L \bar{W} = \rho_r S_T = \rho_r S_L \frac{A_L}{A_T} \tag{6}$$

where

$$\overline{W} \equiv \int_0^\infty \frac{\nu(\xi)}{U_n(\xi)}\, d\xi \qquad (7)$$

Note that $\overline{W}$ which is the ratio between the turbulent burning rate and the laminar burning rate is identical to the increase in flame area due to turbulence A_L/A_T and the turbulent/laminar burning speed ratio S_T/S_L. The objective of our study, therefore, is to develop a experimental procedure to verify Eq. (6) in simple laboratory flame configurations.

EXPERIMENTAL SET-UP AND DATA ANALYSIS

The two configurations used in this study are 1) rod-stabilized oblique v-flames [6,7,10] and 2) large Bunsen conical flames [8]. The diameter of the CH_4/air jet for both burners is 50 mm. The v-flame is surrounded by an outer co-flow air jet of 100 mm. The conical flame is stabilized by a ring of premixed methane/air pilot flames. Incident turbulence is generated either by a square grid ($u' = 5\%$) or a perforated plate ($u' = 8\ \%$) placed 50 mm upstream of the exit. Other details of the experimental set-ups and data acquisition system are reported in previous papers [6-10]. Flow and mixture conditions for the five v-flames and four conical flames are shown in Table I. Under these conditions, the integral scale Reynolds number, Re_l, and the Damkohler numbers, Da, show that the turbulent flames studied here fall within the wrinkled laminar flame regime.

The flame crossing frequencies ν are measured by monitoring the Mie scattering from a silicone aerosol introduced into the reactant stream. This is the same seeding technique used to measure conditional reactant velocities and for two dimensional tomographic imaging. The technique is based on the principle that the oil droplets evaporate and burn at the thin flame front. As shown in Fig. 1, transitions of the Mie scattering signal from burned to unburned states are sharp, therefore the data for $\overline{t}_r$ and $\overline{t}_p$ are relatively insensitive to the choice of the threshold. It has been used recently for measuring the probability density distributions (pdf) of $\overline{t}_r$ and $\overline{t}_p$ with satisfactory results[14].

Since our analysis involves integrating the experimental data through the flame brush, the measurement trajectories is important. In the past, data have been obtained along fixed vertical or transverse axes in laboratory coordinates. This was due mainly to limitations in the traversing mechanism for the diagnos-

tic probe. Except for the centerline along the conical flame, these traverses have no physical significance to the flow paths through the flame brush. The present analysis, as shown by Eq. (5), is valid for properties along streamlines, therefore the logical choice is to measure along the mean flowlines i.e. the Lagrangian lines of the turbulent flames. Using a computer controlled data acquisition system interfaced with a three dimensional traverse laser table and a two component laser Doppler anemometry (LDA) system, it is possible to trace automatically a flowline as specified by the local two dimensional unconditioned velocity vector, $\vec{U}$. The unconditioned velocity components are measured using refractory Al_2O_3 particles. From a starting point x_0 and y_0 within the reactants, the system determines the next measurement position by measuring and computing the mean velocity components $\overline{U}$ and $\overline{V}$, then moves the LDA probe by a fixed increment in the direction of $\vec{U}$. The flowline locations through the flame zone are recorded and stored for measuring the $\nu(\xi)$ and $\overline{c}(\xi)$ profiles.

There are several diagnostic methods such as the two point Rayleigh scattering technique [15] and the multi-point ion current probes technique[16] suitable for measuring U_n of Eq. (4). Their major drawback is that the analysis of the results are time consuming and not very convenient for collecting large amount of data. Studies in v-flames[15,17] and large conical flames[16] have shown that the flamelets move at speeds close to the that of the mean incident flow since the propagation speed of the flamelets into the reactants is small compared to the mean flow convection speed. This implies that the absolute magnitude of the conditioned velocity in the reactants $|\vec{U}_r|$ is a fair approximation for U_n. As in our previous work, the $|\vec{U}_r|(\xi)$ are measured using silicone oil aerosol as the LDA seed.

The LDA is a four-beam two color system with all four beams frequency shifted by Bragg cells to remove directional ambiguity[9]. It measures simultaneously the velocity components parallel (U) and perpendicular (V) to the burner axis using a 10 μsec covalidation criterion. The Doppler bursts are analyzed by two frequency counters. At each measurement position, 8192 pairs of velocity data are recorded. The biasings on the unconditioned velocity statistics due to uneven seed densities in the burned and the unburned zones are corrected by using the time between data weighted averaging technique.

The experimental arrangement of the Mie scattering technique is identical to that of the single point Rayleigh scattering [15]. Mie scattering intensity from the 488 nm blue light is collected by a photomultiplier assembly focussed on the waist of the laser beam. Spatial resolution is controlled by an adjustable slit. The output signal is digitized at 5 or 10 kHz and the mean values of c and ν are deduced using 40960 samples. Although the results are insensitive to the exact value of the threshold, occasional shot noise from the unburned state may create virtual flame crossing if the threshold is set too close to $\overline{c} = 0$. Consequently, a threshold of $\overline{c} = 0.75$ is used for all the analysis.

RESULTS

For each flame, measurements were made along two flowlines initially at $y_0 = 10$ and 20 mm from the centerline. In addition, traverses along the centerlines of the conical flame were also made. The flowlines determined for flames V1 and C3 are shown in Fig. 2. Also shown are the contours $\overline{c} = 0.1$ and 0.9 to outline the overall orientation of the turbulent flame brushes. In the v-flame, the two flowlines have similar features with an outward deflection in the reactants and then a turn towards the centerline on passing through the flame zone. In the conical flames, due to flow constraints imposed by the flame cone envelope, flow deflection does not occur in the reactants. Along the oblique flame region above the stabilization region, flow deflection is significant in the products and becomes less significant towards the flame tip.

Note that for both flames, the flame angles are very oblique to the flowlines. As the conventional definition of S_T is the velocity component normal to the flame brush, it can be seen that the uncertainties of the results would be large since it involves subtracting the angle between the flowline and the flame orientation. Fig. 2 (b) also shows another problem arising from the application of the flame orientation method to conical flames. Since the flow is normal to the flame brush at the centerline, this technique suggests that S_T is there equal to U_∞ [11].

The mean profiles of $\overline{c}(\xi)$, $\nu(\xi)$, the magnitudes of the conditioned and unconditioned velocity vectors, $|\,\overline{U}_r\,|\,(\xi)$ and $|\,\overline{U}\,|\,(\xi)$, are shown in Fig. 3, and the corresponding turbulent kinetic energies ($q'(\xi)$ and $q'_r(\xi)$) measured in flame V3. The reference point was x_0=32, and y_0=20mm. The $\overline{c}$ profile is

typical of those found in premixed turbulent flames. The ν profile has a maximum of 669 Hz near $\bar{c} = 0.5$. The velocity profiles are similar to those reported previously for transverse axes. $|\tilde{U}|$ increases to a plateau in the products and q' attains a maximum within the flame zone while $|\tilde{U}_r|$ and q'_r remain relatively unchanged. The main difference is that the q' maximum shown here does not correspond to $\bar{c} = 0.5$.

All the $\bar{c}$ profiles are spline fitted to obtain the flame brush thickness δ_T using the maximum gradient method[18]. Listed in Table II are the δ_T results and other parameters deduced from the experimental data. All the δ_Ts are significantly larger than the smaller flame thicknesses typically of 4 to 10 mm determined previously across radial or transverse axes. Therefore, these traverses flame thicknesses can be quite misleading. The data also show the growth of the flame brush from the stabilization region. This is accompanied by a decrease in ν_{max}. This behavior is in accord with Eq. (7) because for $\overline{W}$ to be consistent for a given flame, an increase in δ_T (i.e. a larger region where $\nu/|\tilde{U}_r|$ is non-zero) implies a decrease in ν.

It is also important to note that the parameter $\overline{w}/\rho_r S_L = \nu/|\tilde{U}_r|$ is an inverse length scale which may be interpreted as the average distance between the flamelets. In Fig. 4, the distributions of $\nu/|\tilde{U}_r|$ in $\bar{c}$ space are shown normalized by the integral $\int_0^1 \nu/|\tilde{U}_r| \, d\bar{c}$. The experimental results are compared with the normalized distribution obtained in BLM by solving the ordinary differential equation for $\nu(\bar{c})$.

$$\frac{\overline{w}}{\rho_r S_L} = \frac{\nu(\bar{c})}{U_n(\bar{c})} = \frac{\bar{c}(1-\bar{c})}{U_n T} \tag{10}$$

where T is the scalar integral time scale. The model prediction is symmetrical when U_n and T are assumed to be constant. The experimental profiles are self similar for both the v-flames (Fig. 4(a)) and for the conical flames (Fig. 4(b)). However, all their maxima are skewed towards $\bar{c}$=1. Since the distribution of $|\tilde{U}_r|$ through the flame zone is relatively constant (Fig. 3), the results imply that the scalar time scale decreases as $\bar{c} \rightarrow 1$. This decrease is in agreement with our previous measurement of the time scales along fixed transverse axes[14]. The cause of the decrease is unclear but may be due to the cusps of the flamelets.

The values of $\overline{W}$ listed in Table II were obtained by integrating $\nu/|\tilde{U}_r|$ between the positions $\bar{c} = 0.05$ and 0.95 as, at the edge of the flame zone, the crossing frequencies and their contributions to $\overline{W}$ become very small. Since our sampling time is about 1.6 sec., the uncertainties of the results obtained

there are large.

The $\overline{W}$ results can be compared directly on the conventional S_T/S_L versus q'/S_L plane since $\overline{W} = S_T/S_L$. Shown in Fig. 5(a) is the correlation of $\overline{W}$ in the v-flames with q' at $\bar{c}$=0.05 compared with S_T/S_L in CH_4 / air stagnation point stabilized flames[9] under similar flow conditions. The advantage of the stagnation flow configuration is that at the centerline the flame brush is normal to the approach flow and S_T can be defined unambiguously by the flow velocity entering the flame brush. Also shown are the results determined using the flame orientation method for ethylene/air v-flames[10] and for selected profiles in flames v1 through v5. The various sets of results are fitted linearly by a least mean square.

It is apparent that our $\overline{W}$ results are in good agreement with those of the stagnation point flames. Both sets of data show the same scatter and the difference in the slopes of the linear fit may be attributed to differences in flame geometry. Note that the results determined by the flame orientation method for the the methane/air and ethylene/air v-flames are higher. However, it should be pointed out that the uncertainties associated with the oblique flame data are very large since the method involves determining by subtraction the small angle between the incident flow vector and the flame tangent. The uncertainties estimated in Ref. 10 were about $\pm$ 1.0 S_L. Our $\overline{W}$ data clearly fall within this large error bar. On the other hand, the uncertainties of our present results is much smaller because they are obtained by integration. The uncertainties of $|\vec{U}_r|$ are estimated to be less than 5% while the uncertainties of ν due to variation in the threshold value are about the same order of magnitude. Therefore, the flame crossing frequency method developed here is an attractive viable alternative for determining the turbulent burning speed.

The result obtained in the conical flames are shown in Fig. 5(b). In contrast to the v-flame results, the conical flame results show a consistent trend of increasing $\overline{W}$ towards the flame tip region. This is better illustrated by fitting separately the results obtained on the centerline, at y_0 = 10.0 and 20.0 mm. The profiles with y_0 = 20.0 mm are within the oblique flame zone and closest to the burner rim. These results are consistent with those of the oblique v-flames. Closer to the flame tip, the flame brush are more normal to the approach flow, $\overline{W}$ increases to its maximum value at the centerline. It is interesting to note

that this behavior is similar to the behavior of the laminar burning speed in laminar conical flames[19]. The increase is explained by the effect of flame stretch. At the tip region the flame is compressed (or negatively stretched). Transport of heat to the reactant is increased which enhances the burning rate. Whether this same argument can be used for the turbulent flame data requires more detailed study. However, the most significant aspect of the conical flame results is that prior to this study, the burning speed along the centerline has not been reported because as mentioned earlier the flame orientation method implies that the turbulent burning speed is equal to the approach flow velocity. By using the flame crossing frequency method, we have demonstrated that the turbulent burning rate or speed can be determined with more confidence in complex flame geometries.

DISCUSSION

Having shown that the BCL model for $\overline{w}$ is convenient for determining S_T, it would be useful to examine its physical implications. It is helpful to write Eq. (7) in $\bar{c}$ space by introducing the parameter $d\bar{c}/d\xi$ which is the probability of encountering a flamelet at a given position.

$$\overline{W} \equiv \int_0^\infty \frac{\nu(\xi)}{U_n(\xi)} \frac{d\xi}{d\bar{c}}\, d\bar{c} \tag{11}$$

Since its maximum value at $\bar{c} = 0.5$ is taken to define the inverse of the turbulent flame brush thickness, $1/\delta_T$. Eq. (11) can be interpreted as the ratio between the flame brush thickness and a length scale of the flamelets. It is also illuminating when the models for ν and $d\bar{c}/c\xi$ are introduced into Eq. (11). The model for ν is shown in Eq. (10), and $d\bar{c}/c\xi$ can be approximated by $K\bar{c}(1-\bar{c})/\delta_T$ where K is an empirical constant. The expression for $\overline{W}$ reduces to $\int_0^1 \delta_T/KU_nTd\bar{c}$ which is simply δ_T/KU_nT, where U_nT is the mean spatial scale of the scalar field in the flame region.

This above interpretation again emphasizes the importance of the measurement trajectories. In an analysis similar to the present one, Gouldin and Dandekar[20] estimated S_T of turbulent v-flames by integrating the density pdfs along the y axis. Their results are about 25 times lower than the S_Ts determined by the flame orientation method. This large discrepancy was attributed to streamtube divergence.

However, in the light of the present results, it seems more likely that the discrepancy is caused by the use of transverse density profiles which under estimate the flame brush thickness.

It is then clear that the present analysis which involve transformation of time scales into length scales is restricted by the same criterion as for Taylor's hypothesis. Therefore the method would break down for flames where $u' << | \vec{U}_r |$ is not satisfied. To study this aspect of the model, some flame crossing frequencies obtained in stagnation point stabilized flame [21] were used to estimate $\overline{W}$ according to Eq. (7). Typical Uabsr in the flame zone was about 1.2 m/s compare to 5 to 7 m/s in the v and the conical flames. The estimated $\overline{W}$ were all much lower than the corresponding S_T. This characteristics of the stagnation flow stabilized flame is also considered by Bray, Champion and Libby in their model for these flames [22] where the reaction rate is modified to

$$\overline{w} = \frac{\rho_r S_L \nu(\xi)}{u'(\xi)} \tag{12}$$

where ξ is the co-ordinate normal to the flame brush. To be consistent with our present analysis for two-dimensional flowfields, the more appropriate model should be

$$\overline{w} = \frac{\rho_r S_L \nu(\xi)}{q'(\xi)} \tag{13}$$

The $\overline{W}$ results obtained by Eq. (13) for two flames are also shown in Fig. 5(b). They are more in accord with the S_Ts determined by the flame geometry method. Since the stagnation flow stabilized flame configuration is considered to be closest to the idealized normal flame, further investigation of the flame crossing frequencies and their relationship to the model of $\overline{W}$ for this configuration is needed. In particular, direct measurement of the length scale by a multi-point diagnostic techniques such as tomography is essential. However, for other configurations where Taylor hypothesis is appropriate, the method introduced in this work is a convenient means to determine the burning rate in more complex flame geometries.

By demonstrating that the turbulent burning speed can be deduced from the flame crossing frequencies, we have confirmed the physical significance of the Bray-Champion-Libby model. However, in terms of improving the predictive capability of the present model, our results have indicated that the peak flame crossing frequencies are coupled with the flame brush thickness. To predict the proper burning rate or

burning velocity using the BCL approach seems to require modeling the peak flame crossing frequency, the ν distribution in $\overline{c}$ space and also closing the conservation equation for $\overline{c}$. The $\overline{c}$ conservation equation predicts the flame thickness and is considered in the model of Anand and Pope [4]. It is hoped that further analysis of the data will be helpful in developing closure techniques for the scalar conservation equation and the flame crossing frequencies.

CONCLUSIONS

An experimental procedure has been developed to determine the reaction rate $\overline{w}$ in premixed turbulent flames. It utilizes the Bray Champion and Libby[13] model for turbulent flames consisting of unstrained or equally strained flamelets. The reaction rates were determined by measuring flame crossing frequencies and unconditioned velocity statistics of two components. A method of analysis has also been developed to deduce the turbulent burning speed S_T from $\overline{w}$ data. The most important requirement of the method is that for applications to oblique flames, the measurements be made along mean Lagrangian flowlines. Otherwise the burning rate would be seriously under estimated. A computer controlled two-component LDA system was used to trace the flowlines through the flame brush.

The method has been applied to study five turbulent v-flames and four turbulent conical flames all using methane/air mixtures. For each flame, measurements were made along at least two flowlines. The distributions of $\overline{w}$ in $\overline{c}$ space are self similar and independent of flame configuration. Compared to the symmetric distribution predicted by the model, the experimental data have maxima skewed towards the burned side ($\overline{c} > 0.5$) implying a decrease in the length scales not predicted by the present model.

The S_T results obtained by integrating $\overline{w}$ along a 2D mean flowline are in excellent agreement with those obtained in the stagnation flow stabilized flame and in the v-flames. The S_Ts for the conical flames show slight increases toward the flame tip region whereas the v-flame results seem to be independent of the position. These results confirm the physical significance of the BCL reaction rate model and also demonstrate that the proposed method is an attractive alternative for determining the turbulent burning speed. Compared to the flame orientation method, its uncertainties are much lower and, more importantly, it can be applied to study flames with more complex and ambiguous geometries such as through the centerline of

the conical flames.

NOMENCLATURE

$\bar{c}$	progress variable
Da	Damkohler number
q'	turbulent kinetic energy $\equiv 1/3 \sqrt{u' + 2v'}$
l_x	integral length scale
Re	Reynolds number
S_L	laminar burning speed
S_T	turbulent burning speed
$\lvert \bar{U} \rvert$	absolute magnitude of the velocity vector $= \sqrt{\bar{U}^2 + \bar{V}^2}$
U, u'	mean and rms axial velocity
V, v'	mean and rms radial velocity
$\bar{w}_f$	local product creation rate
$\bar{w}$	local rate of reaction
$\bar{W}$	ratio of turbulent/laminar burning rates
x	axial distance
y	radial or transverse distance
ϕ	equivalence ratio
ν	flame crossing frequency
ρ	gas density
τ	heat release parameter
ξ	co-ordinate along flowline

Subscripts

L	laminar condition
T	turbulent condition
o	reference position for traverse
p	conditioned products properties
r	conditioned reactants properties
∞	free stream

ACKNOWLEDGEMENTS

The authors would like to thank Prof. Bray, Dr. Champion, and Prof. Libby for sharing with us their results prior to publication. The authors would also like to acknowledge Mr. Gary Hubbard for developing the data acquisition and analysis software. This work was supported by the Director, Office of Energy Research, Office of Basic Energy Sciences, Chemical Sciences Division of the U. S. Department of

Energy under Contract No. DE-AC-03-76SF00098.

REFERENCES

(1) Bray, K. N. C., Libby, P. A., and Moss, J. B.: *Comb. Sci. Tech., 41,* 143 (1984).

(2) Bray, K. N. C., and Libby P. A.: *Comb. Sci. Tech., 47,* 253 (1986).

(3) Peters, N.: *21st Symposium (International) on Combustion,* (1986).

(4) Anand, M. S., and Pope, S. B.: *Combst. Flame, 67,* 127 (1987).

(5) Gouldin, F. A.: *Combst. Flame, 68,* 249 (1987).

(6) Cheng, R. K.: *Comb. Sci. Tech., 41,* 109 (1984).

(7) Cheng, R. K., and Shepherd, I. G.: *Comb. Sci. Tech., 49,* 17 (1986).

(8) Cheng, R. K. and Shepherd, I. G.: *Comb. Sci. Tech., 52,* 353 (1987).

(9) Cho, P., Law, C. K., Hertzberg, J. H. and Cheng, R. K.: *21th Symposium (International) on Combustion,* p. 1493, The Combustion Institute, 1986.

(10) Cheng, R. K., and Ng, T. T.: *Combust. Flame, 57,* 155 (1984).

(11) Fox, M. D. and Weinberg, F. J.: *Proc. Roy. Soc. Lond. A, 268* 222 (1962).

(12) Abdel-Gayed, R. G. and Bradley, D.: *16th Symposium (Int'l) on Combustion,* p. 1752, The Combustion Institute, 1977.

(13) Bray, K. N. C., Champion, M. and Libby, P. A.: Submitted to *22nd Symposium (Int'l) on Combustion* (1988).

(14) Shepherd, I. G. and Cheng, R. K.: To be published *Comb. Sci. Tech.*, 1988.

(15) Namazian, M, Talbot, L., Robben, F., and Cheng, R. K.: *19th Symposium (International) on Combustion,* p. 487, The Combustion Institute, 1982.

(16) Suzuki, T. and Hirano, T.: *20th Symposium (Int'l) on Combustion,* p. 437, The Combustion Institute, 1984.

(17) Yoshida, A. and Tsuji, H.: *19th Symposium (Int'l) on Combustion,* p. 403, The Combustion Institute, 1982.

(18) Namazian, M., Shepherd, I. G., and Talbot, L.: *Comb. and Flame, 64,* 299 (1986).

(19) Mizomoto, M.,, Asaka, Y., Ikai, S. and Law, C. K.: *20th Symposium (Int'l) on Combustion,* p. 1933, The Combustion Institute, 1984.

(20) Gouldin, F. A., and Dandekar, F. V.: *AIAA J., 22,* no. 5, 655 (1984).

(21) Cho, P., Law, C. K. and Cheng, R. K.: Stabilized in a Stagnation Flow." Paper 1B-009 presented at the Joint Conference, Western States and Japanese Sections of the Combustion Institute, Nov. 22-26 ,1987.

(22) Bray, K. N. C., Champion, M., and Libby, P. A.: Submitted to *Comb. Sci. Tech.* (1988).

TABLE I Mixture and flow conditions

No.	Config.	U_∞ m/s	u'_∞ %	ϕ	τ	l_x mm	Re_l	Da
V1	v-flame	5.0	8	1.0	6.5	3.0	36	59
V2	v-flame	5.0	8	0.7	5.2	3.0	31	20
V3	v-flame	5.0	8	0.85	5.8	3.0	33	33
V4	v-flame	5.0	5	0.83	5.8	2.0	17	31
V5	v-flame	7.0	5	0.7	5.2	2.0	26	11
C1	conical	5.0	8	1.0	6.5	3.0	37	57
C2	conical	5.0	8	0.85	5.8	3.0	37	30
C3	conical	5.0	8	0.7	5.2	3.0	37	17
C4	conical	7.0	8	0.7	5.2	3.0	43	14

TABLE II Turbulent burning rates and relevant parameters

No.	y_o	*Properties at* $\overline{c} = 0.05$				$\nu_{\max}$	δ_T	$\overline{W}$	$S_T = \overline{W}^* S_L$
	(mm)	x (mm)	y (mm)	q' (m/s)	q'/S_L	Hz	(mm)		(m/s)
V1	10	29.00	13.95	0.190	0.480	722	24.8	2.70	1.08
	20	51.70	27.80	0.184	0.460	641	37.7	3.20	1.28
V2	10	47.00	15.48	0.157	0.790	705	35.4	3.66	0.73
V3	10	30.00	13.26	0.162	0.529	814	20.7	2.50	0.76
	20	52.00	26.10	0.182	0.595	669	30.4	3.06	0.94
V4	10	31.42	14.26	0.132	0.431	804	18.8	2.55	0.78
	20	51.00	24.67	0.140	0.456	650	28.1	2.85	0.87
V5	10	48.75	15.64	0.205	1.025	1008	51.3	5.55	1.11
	20	57.50	18.65	0.197	0.985	979	46.5	5.24	1.05
C1	00	70.00	00.00	0.167	0.418	536	41.8	3.66	0.61
	10	47.50	11.10	0.192	0.480	496	38.8	3.25	1.30
	20	15.84	20.45	0.222	0.555	882	15.2	2.79	1.12
C2	00	69.25	00.00	0.173	0.541	571	41.4	3.79	1.21
	10	45.88	10.92	0.190	0.594	513	36.5	3.30	1.06
	20	15.00	20.00	0.208	0.650	853	16.7	3.25	1.04
C3	00	80.00	00.00	0.161	0.805	538	63.0	5.39	1.08
	10	60.00	10.00	0.172	0.860	514	57.4	5.03	1.01
	20	13.75	20.26	0.233	1.165	913	24.4	4.94	0.99
C4	00	85.00	00.00	0.175	0.875	715	73.6	6.21	1.24
	10	70.84	10.05	0.210	1.050	736	49.3	5.75	1.15
	20	22.50	20.46	0.287	1.435	1109	31.0	4.96	0.99

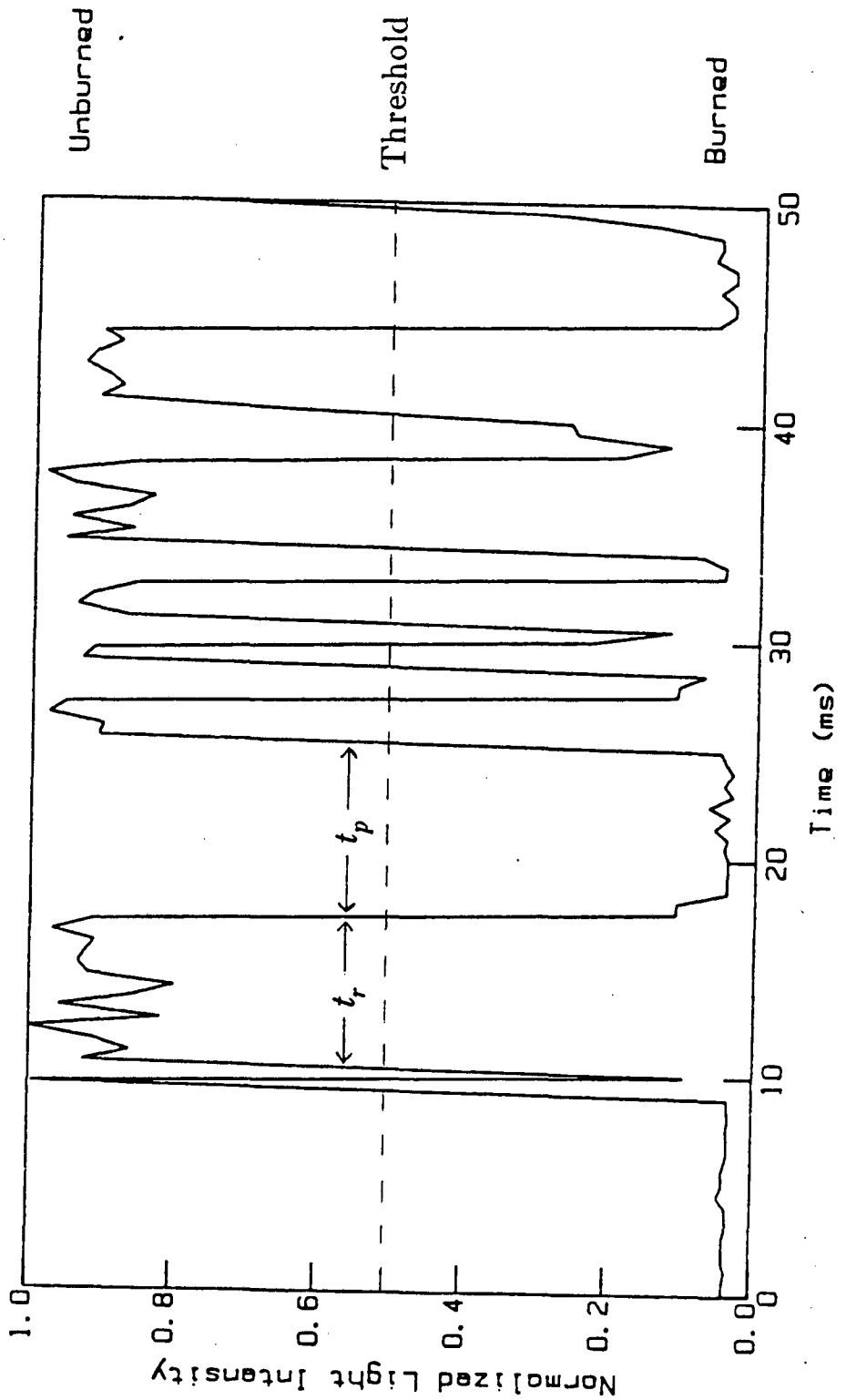
Unburned
Threshold
Burned
t_p
t_r
Normalized Light Intensity
Time (ms)
0.0
0.2
0.4
0.6
0.8
1.0
0
10
20
30
40
50

Fig. 1

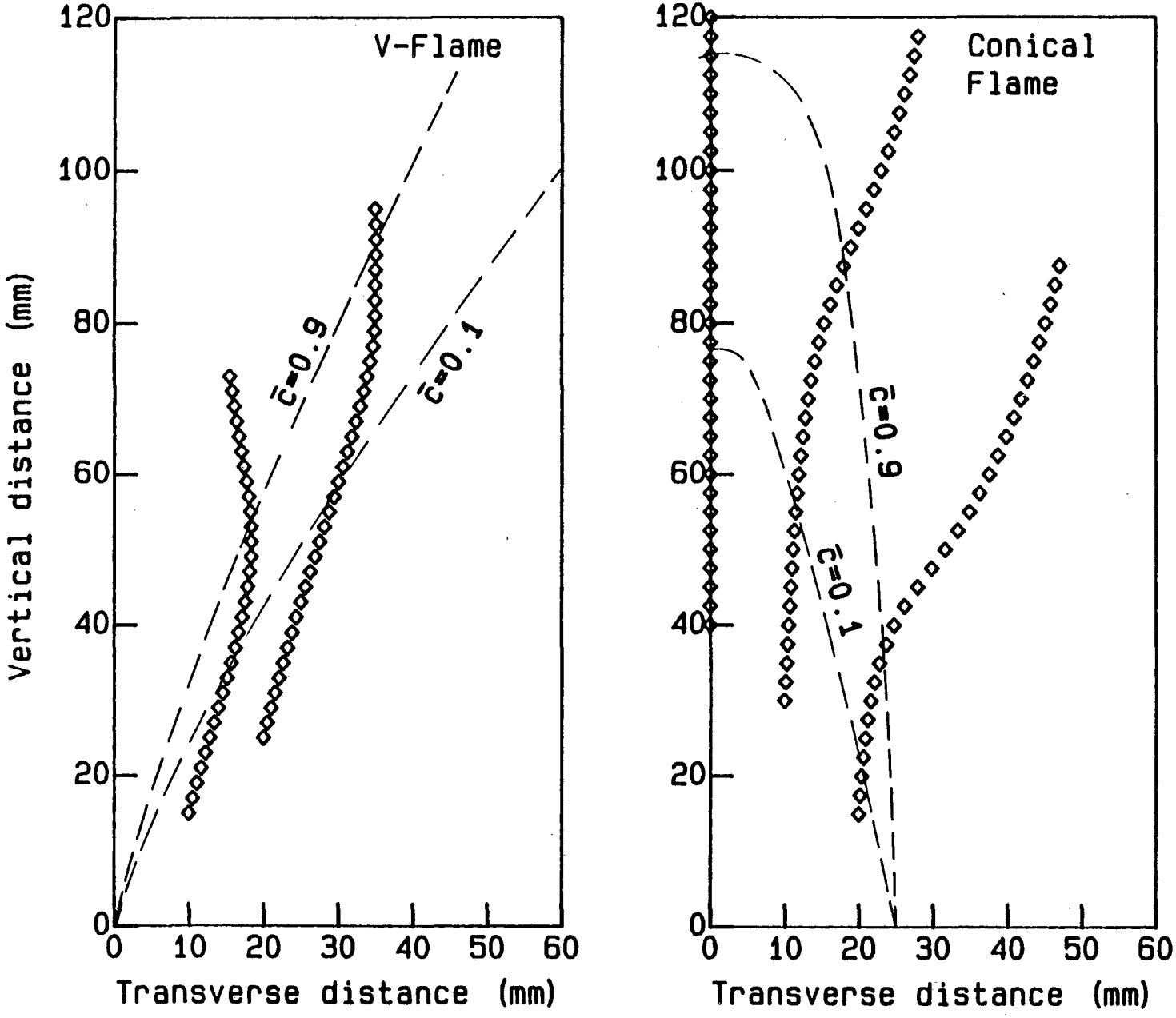
V-Flame
Conical Flame
Vertical distance (mm)
Transverse distance (mm)
Transverse distance (mm)
$\bar{c}$=0.9
$\bar{c}$=0.1
$\bar{c}$=0.9
$\bar{c}$=0.1
0
20
40
60
80
100
120
0
10
20
30
40
50
60

Fig. 2

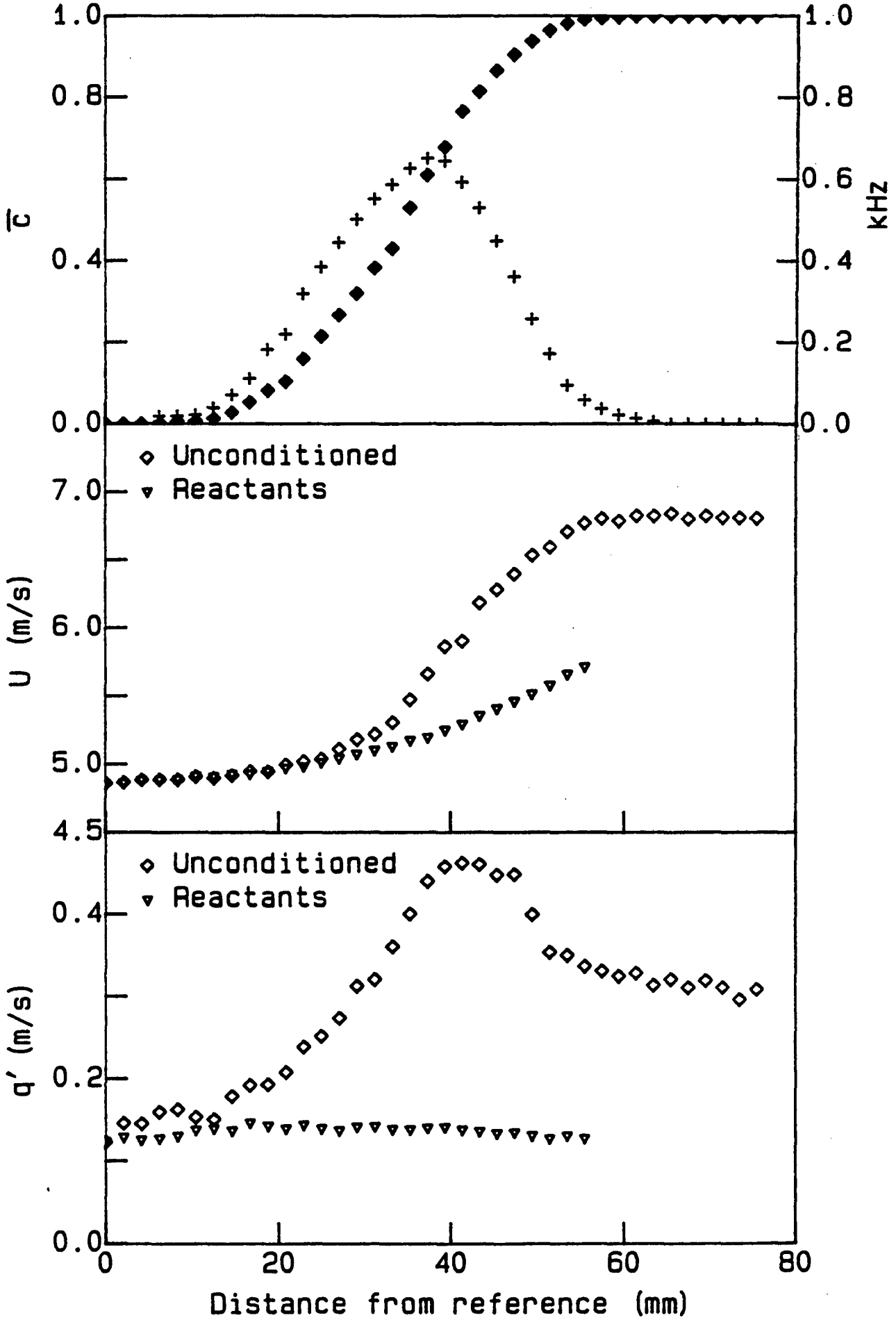
1.0
0.8
0.4
0.0
$\overline{c}$
0.6
0.2
kHz
Unconditioned
Reactants
7.0
6.0
5.0
4.5
U (m/s)
0.4
0.2
0.0
q' (m/s)
0
20
40
60
80
Distance from reference (mm)

Fig. 3

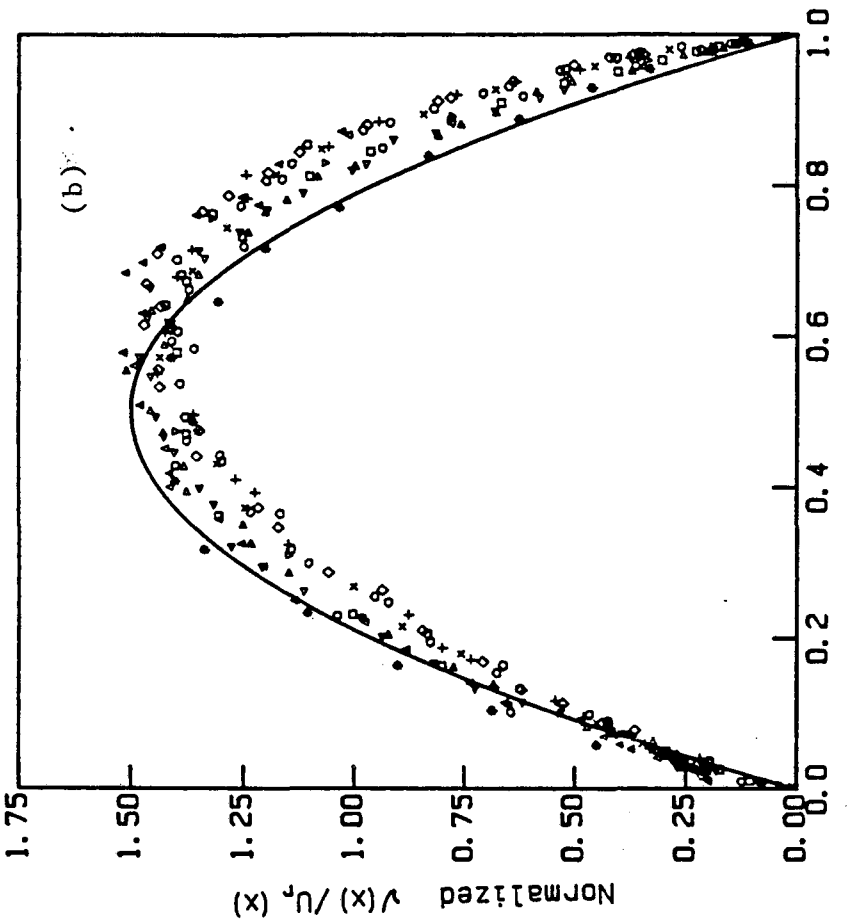
(b)
Normalized v(x) /U_r (x)
1.75
1.50
1.25
1.00
0.75
0.50
0.25
0.00
0.0
0.2
0.4
0.6
0.8
1.0
c̄

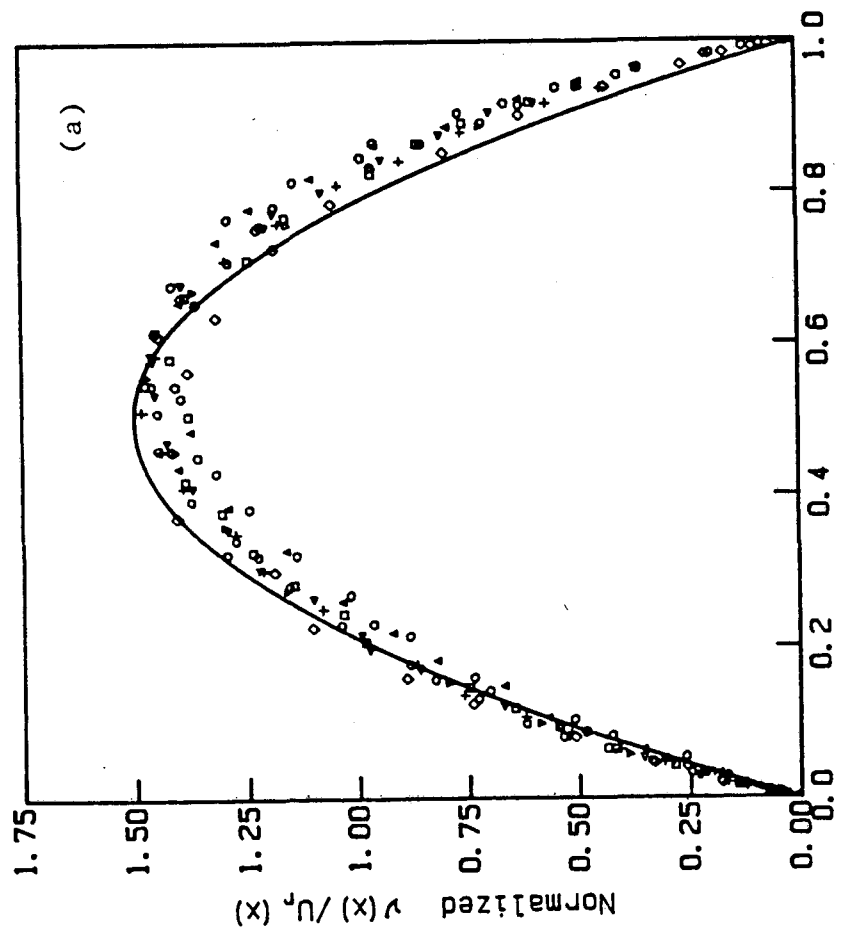
(a)
Normalized v(x) /U_r (x)
1.75
1.50
1.25
1.00
0.75
0.50
0.25
0.00
0.0
0.2
0.4
0.6
0.8
1.0
c̄

Fig. 4

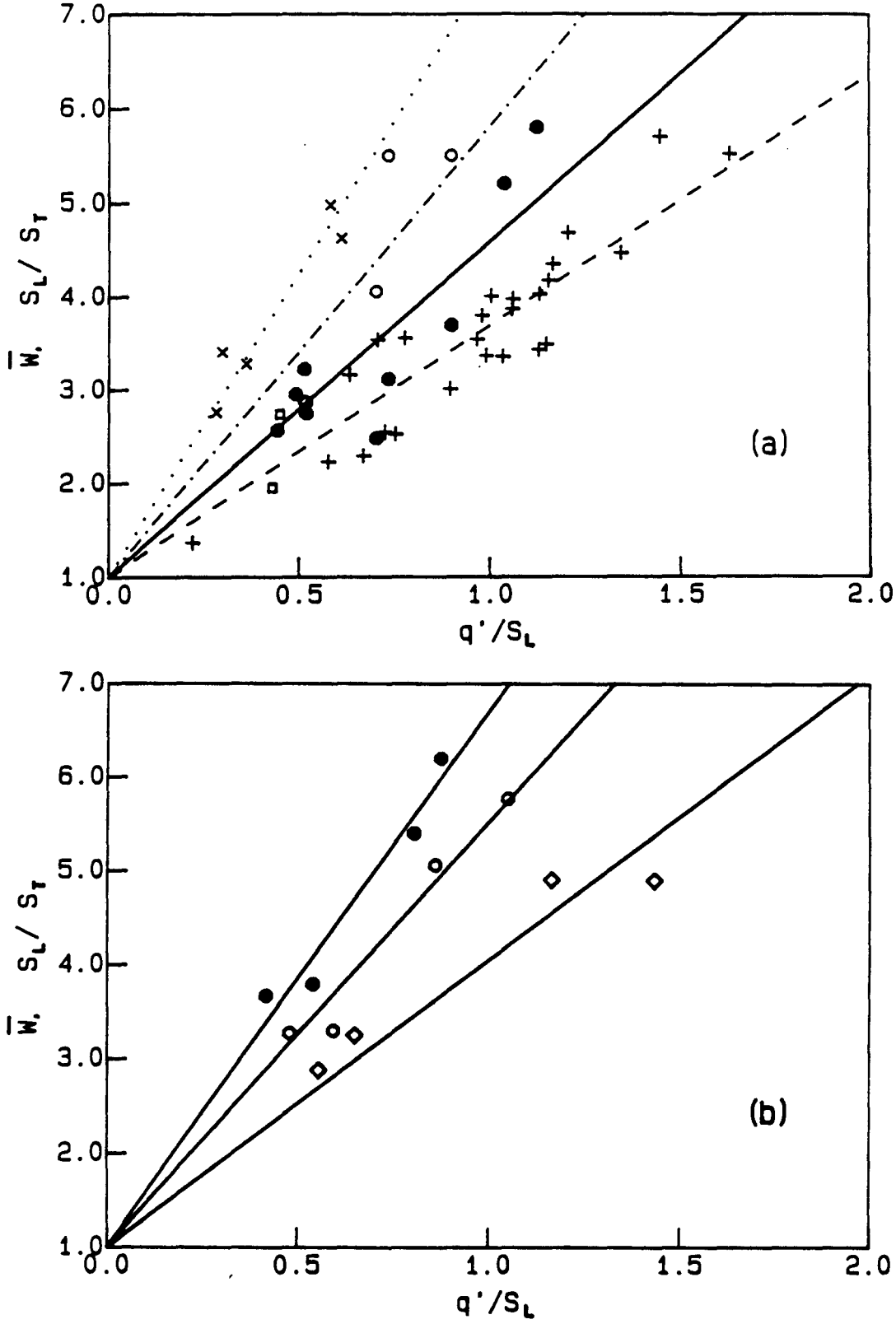

Fig. 5

LAWRENCE BERKELEY LABORATORY
TECHNICAL INFORMATION DEPARTMENT
UNIVERSITY OF CALIFORNIA
BERKELEY, CALIFORNIA 94720